ELSEVIER

International Journal of Mass Spectrometry 192 (1999) 437–444

International Journal of Mass Spectrometry

# Beam capillary spectroscopy

Yasunori Yamazaki

*Institute of Physics, University of Tokyo, Komaba, Meguro-ku, Tokyo 153-8902, Japan and RIKEN, 2-1 Hirosawa, Wako, Saitama 351-0198, Japan*

Received 3 March 1999; accepted 17 May 1999

**Abstract**

In this short article, several recent findings on the interaction of slow highly charged ions with surfaces studied with thin microcapillary foils are discussed, which enables for the first time to extract atoms (ions) in highly and multiply excited states into vacuum, and to study the intrinsic nature of hollow atoms (ions) formed above a surface (HAA). It was found that observed charge-changed fractions were consistent with the prediction of the classical over barrier model. X-ray measurements revealed that a considerable fraction of charge changed ions are in metastable states though keeping multiple electrons in outershells and at the same time keeping innershell hole(s), i.e. metastable multiply excited Rydberg states are formed, which have lifetimes of ~1 ns or longer. Spin-aligned states with less than half-filled shells and/or a highly excited high angular momentum state are possible first order models that explain such an extreme metastability. Visible light measurements, on the other hand, provide detailed information on electrons in highly excited states, e.g. $\Delta n = 1$ transitions from states with $n \sim q$ ($n$ is the principal quantum number of the active electrons, and $q$ the incident charge state) were observed, which proves that electrons on HAA are in high Rydberg states having principal quantum numbers around those predicted by the classical over barrier model, and further, the angular momentum quantum numbers are very high, which is again qualitatively explained with a classical picture. It is emphasized that the combination of slow highly charged ions and capillary foils provides a unique chance to study spectroscopic natures of HAA. (Int J Mass Spectrom 192 (1999) 437–444) © 1999 Elsevier Science B.V.

*Keywords:* Slow highly charged ions; Hollow ions; Primordial distribution; Microcapillary; Classical over barrier model

## 1. Introduction

When a slow multiply charged ion approaches a surface, electrons are resonantly and multiply transferred from the target valence band into excited states of the ion still preserving many holes in inner bound states. Such states are called a hollow atom (ion) above surface (HAA), a new type of atomic state.

Due to the interaction of the ion with its image charge, the ion is accelerated toward the surface until it is neutralized. The time interval $\tau_r$ between the HAA formation and its arrival at the surface is estimated to be $10^{-14}$–$10^{-13}$ s at the longest, which is possibly shorter than its intrinsic lifetime, i.e. it is difficult to study the nature of HAA as far as a flat surface target is used. When the innershell holes are deep enough, they survive for a finite time even if the ion jumps into the sea of valence electrons of the target, although electrons in highly excited states that characterize HAA have already been lost. Such a state is referred to as a hollow atom below surface (HAB). It is noted that the key parameter to govern the HAA

E-mail: yasunori@phys.c.u-tokyo.ac.jp


*PII* S1387-3806(99)00105-0

formation process is the charge state $q$, which is in good contrast with the neutralization of singly charged ions in front of a surface where the energy level matching between the electronic states before and after the transfer plays a decisive role.

The formation and decay dynamics of HAA as well as HAB have been studied intensively in recent years through measurements of charge state and angular distributions of the ions, x rays and Auger electrons, sputtering, etc. [1–10]. Although various exotic features are expected for HAA, their investigation has been quite difficult because the existing time above surface is very limited and signals from HAB are normally much stronger than those from HAA.

The classical over barrier model [11,12] predicts that resonant charge transfer starts at a critical distance $d_r \sim (2q)^{1/2}/W$ into highly excited states with their principal quantum number $n_r$ given by

$$n_r \sim \frac{q}{[2W(1 + (q/8)^{1/2})]^{1/2}} \quad (1)$$

where $q$ is the ion charge and $W$ is the binding energy of the target valence electrons (physical quantities are given in atomic units unless otherwise noted). It is noted that the radii of the resultant excited states are comparable to $d_r$, and accordingly the electrons can move back and forth between the ion and the target when they are in resonance, i.e. HAA in front of the surface is in reality a "dynamic hollow molecule" rather than an atom.

In the present article, a new technique to probe isolated HAA is discussed, which may be called "beam capillary spectroscopy" (BCS) [13–17].

## 2. Microcapillary

Information on the character of HAA has been very limited, which was obtained through measurements of projectile Auger electrons [2] and/or x rays [18] under glancing scattering configurations or under slow ion impacts [5]. As is discussed in Sec. 1, the image acceleration limits the survival time of HAA, although their intrinsic lifetimes could be much longer. After the ion hits the surface, the HAA is then turned into HAB, which also emit Auger electrons and x rays. Accordingly, there exists two major difficulties in studying HAA under conventional experimental arrangement, i.e. signals from HAA are fairly weaker than those from HAB, and the survival times of HAA are possibly too short for their intrinsic nature to be studied.

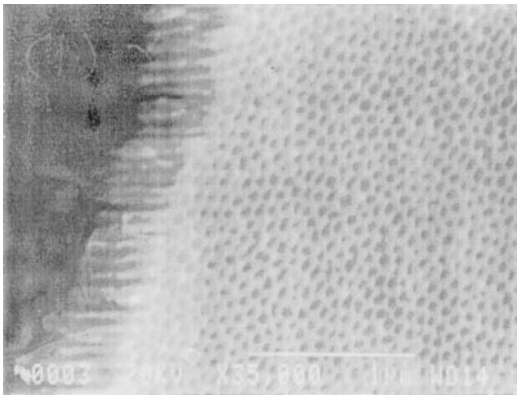

Fig. 1. A SEM image of a typical Ni capillary foil.

A trick to overcome the above mentioned difficulties and to preferentially prepare HAA suppressing signals from HAB is to use a thin foil with straight multimicrocapillaries [19,20]. When HCIs impinge on the target in parallel with the capillary axis, a part of the HAA formed in the capillary can pass through it before hitting the capillary wall. In this case, free HAAs are extracted in vacuum. Fig. 1 shows a scanning electron microscope (SEM) image of a Ni capillary foil with the thickness and the capillary diameter of about 1 $\mu$m and 100 nm, respectively [20]. It is seen that the capillaries are distributed regularly with a honeycomb structure. Considering that ions passing near the capillary wall at a distance shorter than $d_r$ are expected to capture electrons resonantly into their excited states, the charge changed fraction is estimated to be $\sim 2d_r/r$, where $r$ is the capillary radius, which was found to be consistent with the observation. Furthermore, the charge state distribution of the charge changed fraction after the capillary transmission, $f(q)$, depended weakly on $q$ [15], which is very different from that of ions transmitted through a foil or that of specular reflected ions

from a surface [21,22]. In the latter two cases, only neutral and low charge state ions are the major components. The capillary target is an effective and unique material supplying some limited number of electrons keeping the charge state distribution away from the equilibrium. A theoretical study on the interaction of HCI with microcapillaries has just started, which is expected to enhance the activity of BCS very much [23].

## 3. Transitions among highly excited states

The critical distance $d_r$, where electron transfers from the target valence band to the excited states of ions become classically allowed, has been demonstrated to have wide applicability in various experiments, e.g. measurements of the angular shift of specular reflected ions under glancing incidence [4], and measurements of velocity dependent secondary electron yields [6], both of which primarily monitor the energy gain induced by the image acceleration which lasts until the ion is neutralized. It is noted that there exists no direct measurement that can determine $n_r$, because the observation time of HAA is fairly limited when a conventional flat surface target is employed. In the case of a capillary target, on the other hand, HAA and its relatives are extracted in vacuum and are isolated, which provides direct information on their initial states.

$n_r$ given by Eq. (1) is plotted by the dotted line for $W \sim 4.5$ eV in Fig. 2 as a function of the charge $q$ of the incident ion. Taking into account the ion velocity $v_p$ along the capillary wall, the transferred electron have, on the average, an additional kinetic energy of $\sim 1/2 m_e v_p^2$ in the projectile frame, i.e. the principal quantum number of the realized states could be larger than $n_r$. The angular momentum $l_m$, which is crudely estimated by $\sim m_e v_p d_r$ is also shown by the solid lines in Fig. 2 for six different ion velocities ranging from 0.1 to 1.1 a.u., which tells that $l_m$ is comparable to $n_r$ under the conditions discussed here, i.e. Yrast states could be heavily populated. The radiative lifetimes of Yrast states are fairly long because only $\Delta n = 1$ transitions are allowed, and the transition energy in

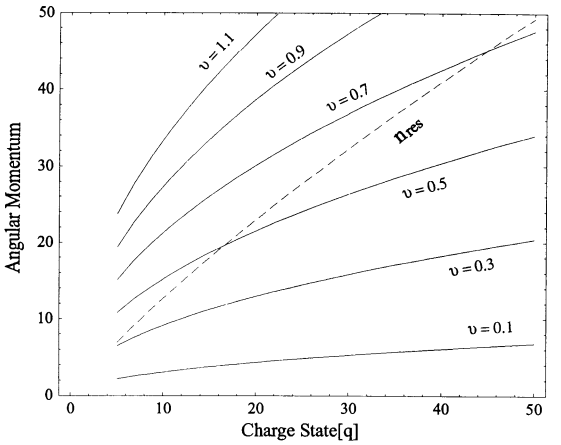


Fig. 2. The angular momentum of transferred electron in the projectile frame for incident ion velocities from 0.1 to 1.1 a.u. (solid lines). $n_r$ [see Eq. (1)] is also plotted assuming $W \sim 4.5$ eV.

the present conditions are in the visible light region as will be discussed. On the other hand, autoionizing transitions to the nearest neighbor states are energetically forbidden because $n_r$ is rather large. A rough estimation indicates that $\Delta n$ should be larger than $\sim 0.3\ n_r$, i.e. large angular momentum changes are also necessary for both electrons involved in the autoionization (the final angular momenta of the autoionizing and the deexciting electrons are $\sim l_m + \Delta n$ and $\sim l_m - \Delta n$, respectively), which will again make the transition rate very small. In other words, the formed states are expected to be highly stable even when electrons are in the same shell, which makes the electron–electron correlation rather strong. In the case of HCI–gas collisions, the velocity dependence of the angular momentum distribution of transferred electrons has been discussed [24,25]. Further, a similar stabilization mechanism is very effective in the case of highly excited $\bar{p}$He, the lifetime of which is known to be longer than 1 $\mu$s [26–28].

Assuming for simplicity one electron is transferred into a high angular momentum state, the transition energy between neighboring states, $\Delta\epsilon_{\Delta n}$, is roughly given by

$$\Delta\epsilon_{\Delta n} \sim \frac{q^2}{2(n_r - \Delta n)^2} - \frac{q^2}{2n_r^2}, \qquad (2)$$

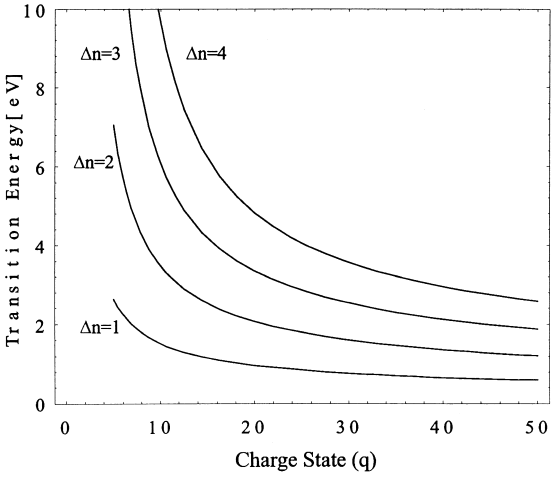


Fig. 3. The transition energy $\Delta\epsilon$ for $\Delta n = 1$, 2, 3, and 4 as a function of charge state $q$ for $W \sim 4.5$ eV (for details see the text).

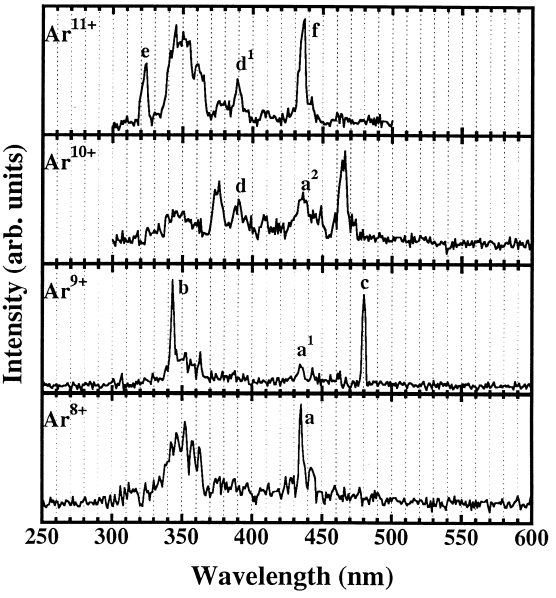


Fig. 4. Visible light spectra observed for incident $Ar^{q+}$ ions of $10q$ keV ($q$ = 8–11) downstream of the capillary target. Top-left corner of the each column shows the incident ions. The spectral resolutions in these observations are about 2.3 nm for $q = 8$ and 9, and 4.5 nm for $q = 10$ and 11.

which is plotted by the solid lines in Fig. 3 for $\Delta n = 1$–4 as a function of $q$, which indicates that many transitions are expected in the visible light region for the experimental conditions considered here. The previous consideration shows that the combination of the capillary target and visible light detection provides the unique chance to directly measure $n_r$ at the beginning of HAA formation.

Observed spectra for $10q$ keV $Ar^{q+}$ ($8 \leq q \leq 11$) incident on the microcapillary target are shown in Fig. 4 [29]. The broad peak around 350 nm seen for all the spectra is attributed to emissions from sputtered Ni atoms [30].

The COWAN code [31] based on a multiconfiguration Hatree-Fock method was used to identify transitions for $q = 8$, 9, and 10 assuming that the incident ion is in the ground state and only one electron is captured into a high Rydberg state which decays through a $\Delta n = 1$ transition. By comparing the observed and calculated transition energies, the peaks $a$, $b$, $c$, $d$, $e$, and $f$ in Fig. 4 are attributed to $9l \rightarrow 8l'(l, l' \geq 5)$ of $Ar^{7+}$, $9l \rightarrow 8l'(l, l' \geq 3)$ of $Ar^{8+}$, $10l \rightarrow 9l'(l, l' \geq 3)$ of $Ar^{8+}$, $10l \rightarrow 9l'$ $(l, l' \geq 2)$ of $Ar^{9+}$, and $10l \rightarrow 9l'$ of $Ar^{10+}$ transitions, respectively. For $q \geq 9$, the incident ions have $L$-shell holes, which makes the electronic configurations fairly complicated, and, in addition, the spectral resolution was lower than that of the incident $Ar^{8+}$, $l$ and $l'$ are rather ambiguous as compared with those of $q = 8$. For $Ar^{11+}$ incidence, the transition energy was calculated assuming Eq. (2).

The peaks $a^1$ and $a^2$ have, in the present spectral resolution, the same wavelength as the peak $a$, and the peak $d^1$ has the same wavelength as the peak $d$. This indicates that the charge states of the ionic cores at the moment of the transitions are $Ar^{8+}$ for $a^1$ and $a^2$, and $Ar^{10+}$ for $d^1$, which are formed via multielectron transfers followed by autoionizations. The peak $f$ could either be attributed to $11l - 10l'$ of $Ar^{10+}$ or $9l - 8l'$ of $Ar^{7+}$. As transfers are preferentially into $n_r \sim q$ [see Eq. (1)], and each autoionization emits an electron, $a^1$ and $a^2$ indicate at least two and three electron transfers, respectively.

Summarizing, the visible light measurements revealed that some considerable fraction of the charge changed components are in high $n$ and at the same time in high $l$ states with $n \sim n_r$ as is foreseen with a qualitative discussion according to the classical over barrier model given in this section.

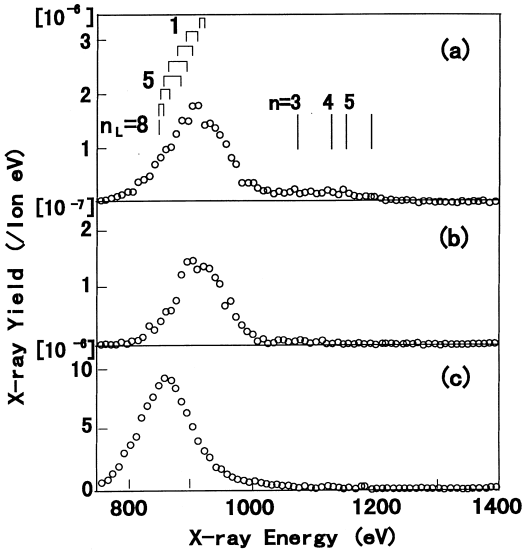


Fig. 5. (a) The energy spectrum of x rays emitted from ions downstream of a Ni microcapillary target for incident 9 keV/u $Ne^{9+}$ ions. (b) The same as (a) except that the delay time is 2.3 ns. (c) The energy spectrum of Ne x rays emitted for an Al plate target. The bars on the left part of (a) show predicted energies of *KL* x rays [32] with the corresponding number of electrons in the *L* shell. The bars in the middle of (a) show the x-ray energies of *np*–1*s* transitions of Ne.

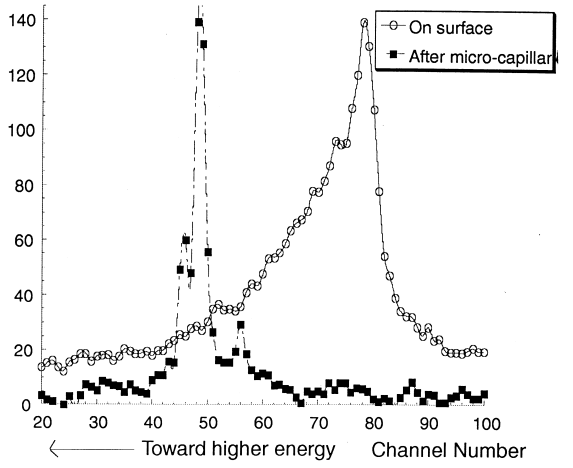


Fig. 6. A high resolution spectrum of Ne *K K* rays emitted when 5 keV/u $Ne^{9+}$ ions are transmitted through the Ni capillary (closed squares), and that with the same ions bombarding a stainless steel plate (open circles). Note that the x-ray energy is higher on the left-hand side.

## 4. Transitions into innershell holes

At some stage, innershell holes are eventually filled via Auger electron emission or via photon emission. In contrast to the visible light measurements, which probe the rather early stages of HAA evolution, the x rays probe somewhat later stage. Fig. 5(a) and (b) show an x-ray energy spectrum observed by a Si(Li) detector for 9 keV/u $Ne^{9+}$ downstream of the Ni capillary target and that delayed by 2.3 ns or longer, respectively [14]. The peak around 900 eV corresponds to *KL* transitions of Ne and the broad bump around 1100 eV observed in Fig. 5(a) corresponds to *KM* and higher transitions. On the other hand, Fig. 5(c) shows an x-ray spectrum observed for the same ion but bombarding an Al plate. In this case, the peak energy is seen about 50 eV lower than that observed for the capillary target. The bars with numbers in Fig. 5(a) show predicted energies of *KL* x rays with corresponding number of electrons in the *L* shell [32]. For the capillary target, there are only a few *L*-shell electrons at the moment of x-ray emission although for the Al plate target, the *L* shell is almost full. The bump at around 1100 eV are barely visible in 5(b), i.e. *KM* and higher transitions decays faster than the *KL* transitions.

The energy resolution of the Si(Li) detector is not high enough to specify the electronic configurations and the number of electrons in outer shells during x-ray emission. In order to determine transition energies more accurately, a grating soft x-ray spectrometer combined with $LN_2$ cooled charge coupled device has been developed [33], which has the energy resolution of ~1.2 eV full width at half maximum at around 300 and ~7.5 eV at 900 eV. The solid squares and open circles in Fig. 6 show the Ne $K\alpha$ x-ray spectrum for 5 keV/u $Ne^{9+}$ transmitted through the Ni capillary and that directly hitting a flat stainless steel plate, respectively [34]. A drastic change in the spectrum structure is seen, which is actually the reason why the 50 eV shift is observed in Fig. 5. The spectrum for the stainless steel target has a high energy tail corresponding to different number of *L*-shell vacancies. It is seen that the spectrum for the capillary target consists at least of three major peaks,

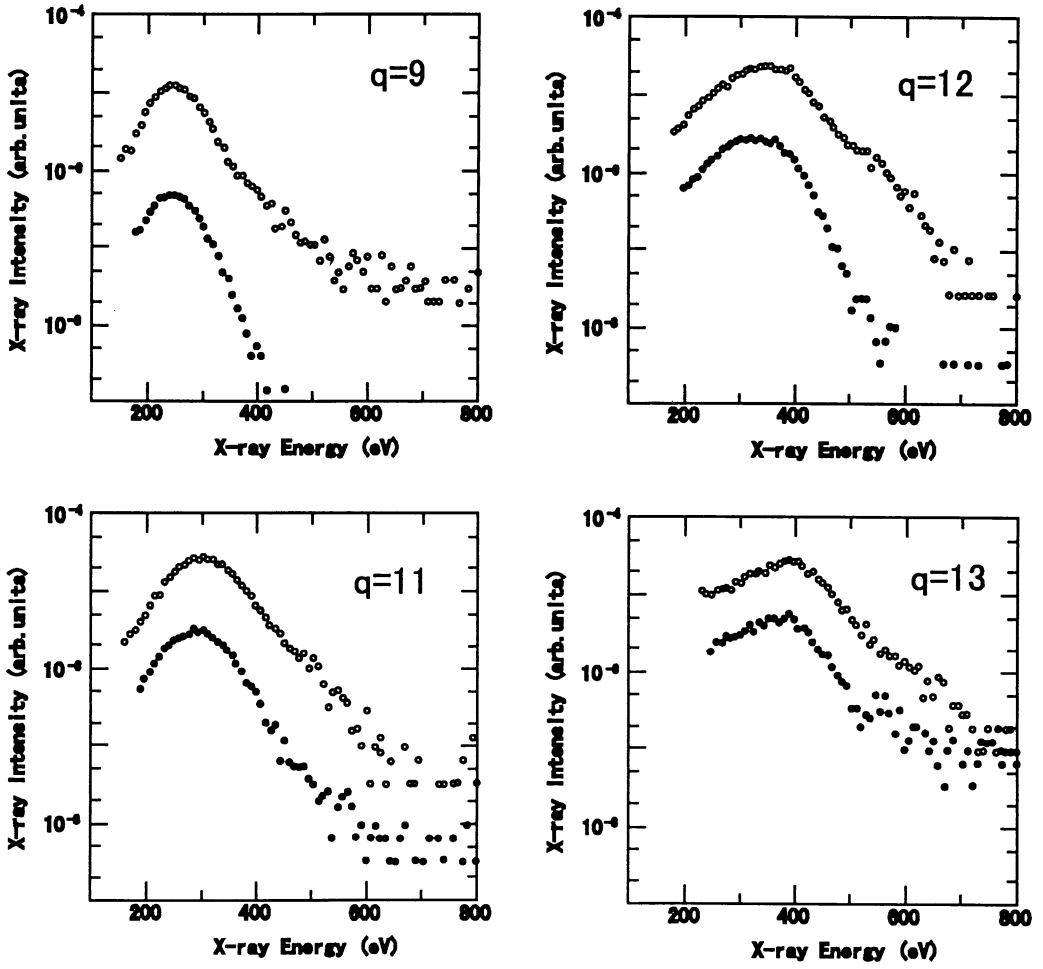


Fig. 7. Energy spectra of Ar $L$ x rays for 3 keV/u $Ar^{q+}$ ions ($q$ = 9–13) incident on a Ni capillary foil measured downstream of the target. For details see the text.

which are at 919.0 ± 1.3, 913.3 ± 1.3, and 894.4 ± 1.3 eV. Comparison with theoretical calculation shows that the core electronic states of the three peaks can be attributed to $1s2p\ ^1P$ (922.1 eV), $1s2p\ ^3P$ (914.9 eV), and $1s2s2p\ ^4P$ (895.0 eV), respectively. The total (radiative and Auger) lifetimes of $Ne^{7+}$ $1s2s2p\ ^4P_{1/2,3/2,5/2}$ states are predicted to be 0.4 (1.6 and 0.43), 0.6 (0.71 and 3.8), and 12 (0 and 12) ns, respectively, which are more or less consistent with the previous observation of 0.8 ns [13]. The observed peak energy of the $1s2p\ ^1P$ on the other hand shows a discernible deviation from the theoretical value although the other two peak energies agree quite well, which indicates contributions from spectator electron(s) located in high Rydberg states.

Fig. 7 shows an x-ray energy spectrum observed by a Si(Li) detector for 3 keV/u $Ar^{q+}$ ($q$ = 9–13) transmitted through the Ni microcapillary target. The open circles are for x rays emitted downstream of the capillary target, and the solid circles are for x rays emitted 3 mm or further downstream of the target, i.e. those emitted ~4 ns or later since the formation of the excited states. The peak around 200–400 eV corresponds to $LM$ transitions of Ar and the high energy

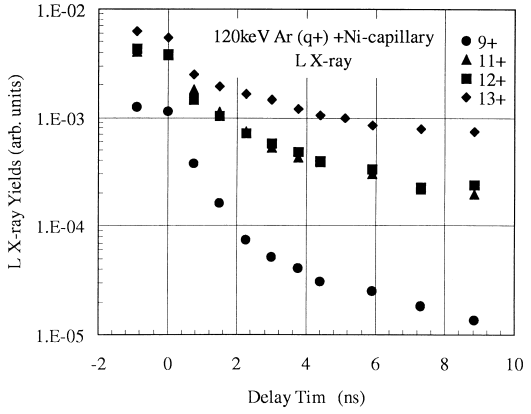


Fig. 8. Ar $L$ x-ray decay curves for 3 keV/u $Ar^{q+}$ ions transmitted through a Ni capillary target.

tail corresponds to transitions from $N$ shell or even higher states. As the traveling time for ions passing through the capillary is $\sim 10^{-12}$ s, excited states which have shorter lifetimes than this do not contribute to the spectra very much. Actually, when the Si(Li) detector is positioned so that it can directly see the inner wall of the capillary, the higher energy tail is considerably enhanced although the peak position stays almost constant. It is seen that (1) the peak energy shifts higher as $q$ increases, (2) the peak positions of the delayed spectra are almost the same for each $q$, i.e. the number of $L$-shell electrons at the moment of $L$ x-ray emission do not vary with time as was also observed for $N^{6+}$ and $Ne^{9+}$ (see also the following).

The decay curves of x rays for 3 keV/u $Ar^{q+}$ ($q$ = 9–13) are shown in Fig. 8. It is seen that (1) each curve consists of at least two components with characteristic times in the range of 1–10 ns, (2) the yield ratio of the slow component to the fast component increases drastically with $q$, which are surprisingly long compared with a typical lifetime of Ar $L$-shell hole.

Such metastability of multiply excited atoms (ions) could be realized if all the spins of bound electrons are aligned, and all the shells are less than half-filled, which is consistent with the observed x-ray energies, indicating a small number electrons in the active shells. It is noted however, that x rays are not only emitted from two or three electron systems but also from five or more electron systems [15], which was proved by employing a delayed coincidence measurements between the exiting charge states and x rays. Further, the coincidence yield is very large, e.g. ~8% and 0.5% for exiting $N^{5+}$ and $N^{2+}$, respectively, again confirming that a distant collision primarily governs the charge transfer in the case of capillary targets.

For the transitions to take place from these spin aligned excited states, mixing of spin-flipped components in the initial and/or the final states of the active electron is essential, which is induced by the $\boldsymbol{l \cdot s}$ interaction. Because the $\boldsymbol{l \cdot s}$ interaction becomes less important for higher excited states, the transitions are more probable from the lowest shells, which is again consistent with the observation. Another possible mechanism of stabilization is the one discussed in Sec. 3, i.e. multiple electrons are stored in highly excited and high angular momentum states, a part of them slowly flows out into the low lying states because of their metastability. Such a situation reminds us of the case of meteors shining above the sky which are stored in the asteroid “reservoir” and leaves their stable orbits from time to time.

## 5. Summary

A new technique to study the interaction of highly charged ions with surfaces have been discussed. The combination of slow highly charged ions and a microcapillary foil is demonstrated to have a high ability to prepare isolated highly and multiply excited metastable atoms (ions) in vacuum. X rays emitted from the metastable states were measured (1) in coincidence with the exiting charge states, which revealed the number of electrons and lifetimes of the atoms (ions), and (2) with a high resolution soft x-ray grating spectrometer, which allows one to identify the core electronic configurations of the atoms (ions). Further, visible light was also measured, which showed that Rydberg states with principal quantum numbers around the incident charge state are heavily populated, which is the first direct evidence that the

states similar to those predicted by the classical over barrier model are really formed. It is discussed that the formation of high spin multiplicity states with less than half-filled shells and/or high angular momentum high Rydberg states is responsible for the stabilization.

## Acknowledgements

The author is deeply indebted to H. Masuda, S. Ninomiya, S. Thuriez, Y. Morishita, and Y. Iwai for their collaboration and fruitful discussions. The research is supported in part by the Grant-in-Aid for Developmental Scientific Research (07555006) from the Ministry of Education, Science, and Culture, and by the President's Special Research Grant of RIKEN.

## References

[1] J.P. Briand, L. de Billy, P. Charles, S. Essabaa, Phys. Rev. Lett. 65 (1990) 159.
[2] F.W. Meyer, S.H. Overbury, C.C. Havener, P.A. Zeijlmans van Emmichoven, D.M. Zehner, Phys. Rev. Lett. 67 (1991) 723.
[3] H.J. Andrae, et al., Z. Phys. D 21 (1991) S135.
[4] HP. Winter, Europhys. Lett. 18 (1992) 207.
[5] J. Das, R. Morgenstern, Phys. Rev. A 47 (1993) R755.
[6] F. Aumayr, H. Kurz, D. Schneider, M.A. Briere, J.W. McDonald, C.E. Cunningham, HP. Winter, Phys. Rev. Lett. 71 (1993) 1943.
[7] R. Koehrbrueck, M. Grether, A. Spieler, N. Stolterfoht, Phys. Rev. A 50 (1994) 1429.
[8] L. Folkerts, S. Schippers, D.M. Zehner, F.W. Meyer, Phys. Rev. Lett. 74 (1995) 2204.
[9] K. Kakutani, T. Azuma, Y. Yamazaki, K. Komaki, K. Kuroki, Jpn. J. Appl. Phys. 34 (1995) L580.
[10] T. Neidhart, F. Pichler, F. Aumayr, HP. Winter, M. Schmid, P. Varga, Phys. Rev. Lett. 74 (1995) 5280.
[11] J. Burgdoerfer, P. Lerner, F.W. Meyer, Phys. Rev. A 44 (1991) 5674.
[12] J. Burgdoerfer, R. Morgenstern, A. Niehaus, J. Phys. B 19 (1986) L507.
[13] Y. Yamazaki, S. Ninomiya, F. Koike, H. Masuda, T. Azuma, K. Komaki, K. Kuroki, M. Sekiguchi, J. Phys. Soc. Jpn. 65 (1996) 1199.
[14] S. Ninomiya, Y. Yamazaki, T. Azuma, K. Komaki, F. Koike, H. Masuda, K. Kuroki, M. Sekiguchi, Phys. Scripta T 73 (1997) 316.
[15] S. Ninomiya, Y. Yamazaki, F. Koike, H. Masuda, T. Azuma, K. Komaki, K. Kuroki, M. Sekiguchi, Phys. Rev. Lett. 78 (1997) 4557.
[16] Y. Yamazaki, Phys. Scripta T 73 (1997) 293.
[17] Y. Yamazaki, invited papers of XXth ICPEAC, Vienna, 1997, Photonic, Electronic and Atomic Collisions, F. Aumayr, HP. Winter (Eds.), World Scientific, Singapore, 1998, pp. 693–702.
[18] B. d'Etat, J.P. Briand, G. Ban, L. de Billy, J.P. Desclaux, P. Briand, Phys. Rev. A 48 (1993) 1098.
[19] H. Masuda, K. Fukuda, Science 268 (1995) 1466.
[20] H. Masuda, M. Satoh, Jpn. J. Appl. Phys. 35 (1996) L126; private communication.
[21] D. Wickholm, W.S. Bickel, J. Opt. Soc. Am. 66 (1976) 502.
[22] F.W. Meyer, L. Folkerts, H.O. Folkerts, S. Schippers, Nucl. Instrum. Methods Phys. Res. B 98 (1995) 441.
[23] K. Toekesi, L. Wirtz, J. Burgdoerfer, Nucl. Instrum. Methods Phys. Res. B, to be published.
[24] J. Burgdoerfer, R. Morgenstern, A. Niehaus, J. Phys. B (1986) L507.
[25] J.H. Posthumus, P. Lukey, R. Morgenstern, J. Phys. B 25 (1992) 987.
[26] T. Yamazaki et al., Nature 361 (1993) 238.
[27] N. Morita et al., Phys. Rev. Lett. 72 (1994) 1180.
[28] R.S. Hayano et al., Phys. Rev. A 55 (1997) 1.
[29] Y. Morishita, S. Ninomiya, Y. Yamazaki, K. Komaki, K. Kuroki, H. Masuda, M. Sekiguchi, Nucl. Instrum. Methods Phys. Res. B, to be published.
[30] N.H. Tolk, D.L. Simms, E.B. Foley, C.W. White, Radiat. Effects 18 (1973) 221.
[31] R.D. Cowan, The Theory of Atomic Structure and Spectra, University of California Press, Berkeley, 1981.
[32] C.P. Bahlla, Phys. Rev. A 122 (1975) 12.
[33] Y. Iwai, Masters Thesis, University of Tokyo, March 1999.
[34] S. Thuriez, Y. Iwai, Y. Kanai, H. Ohyama, R. Hutton, H. Masuda, Y. Yamazaki, Abstracts of the XXIst ICPEAC, Sendai, July 1999, unpublished.